Learning to Coordinate with Humans using Action Features

Mingwei Ma [* 1] **Jizhou Liu** [* 1] **Samuel Sokota** [2] **Max Kleiman-Weiner** [3] **Jakob Foerster** [4]

Abstract

An unaddressed challenge in human-AI coordination is to enable AI agents to exploit the semantic relationships between the features of actions and the features of observations. Humans take advantage of these relationships in highly intuitive ways. For instance, in the absence of a shared language, we might point to the object we desire or hold up our fingers to indicate how many objects we want. To address this challenge, we investigate the effect of network architecture on the propensity of learning algorithms to exploit these semantic relationships. Across a procedurally generated coordination task, we find that attention-based architectures that jointly process a featurized representation of observations and actions have a better inductive bias for zero-shot coordination. Through fine-grained evaluation and scenario analysis, we show that the resulting policies are human-interpretable. Moreover, such agents coordinate with people without training on any human data.

1. Introduction

Successful collaboration between agents requires coordination (Tomasello et al., 2005; Misyak et al., 2014; Kleiman-Weiner et al., 2016), which is challenging because coordinated strategies can be arbitrary (Lewis, 1969; Young, 1993; Lerer & Peysakhovich, 2018). A priori, one can neither deduce which side of the road to drive, nor which utterance to use to refer to ♡ (Pal et al., 2020). In these cases coordination can arise from actors best responding to what others are already doing—i.e., following a convention. For example, Americans drive on the right side of the road and say "heart" to refer to ♡ while Japanese drive on the left and say "shinzo". Yet in many situations prior conventions may not be available and agents may be faced with entirely novel situations or partners. In this work we study ways

that agents may learn to leverage semantic relations between observations and actions to coordinate with agents they have had no experience interacting with before.

To illustrate, consider the following situations where people can figure out how to coordinate without prior shared conventions. Imagine a store that sells strawberries and blueberries. You want to buy strawberries but you don't share any common language with the clerk. You are, however, wearing a red hat and you wave the hat to hint that the strawberries are what you want. The clerk has two baskets of strawberries remaining, and so you raise a single finger to indicate that you only want one of the baskets. The clerk produces a paper and plastic bag and you point to the paper bag to indicate that you want the paper one. These examples are so simple that they seem obvious: the red hat matches the color of strawberries, the number of fingers matches the number of baskets you want, and you extend a finger in the direction of the desired packaging (Grice, 1975). While obvious to people, who rely on a theory-of-mind in understanding others, we show that these inferences remain a challenge for multi-agent reinforcement learning agents.

Figure 1. The "Bouba" (right) and "Kiki" (left) effect.

Less obvious examples are common in the cognitive science literature. Consider the shapes in Fig. 1. When asked to assign the names "Bouba" and "Kiki" to the two shapes, people name the jagged object "Kiki" and the curvy object "Bouba" (Köhler, 1929). This finding is robust across different linguistic communities and cultures and is even found in young children (Maurer et al., 2006). The causal explanation is that people match a "jaggedness"-feature and "curvey"-feature in both the visual and auditory data. Across the above cases, there seems to be a generalized mechanism for mapping the features of the person's action with the features of the action that the person desires the other agent to take. In the absence of norms or conventions, people may minimize the distance between these features when making a choice. This basic form of *zero-shot coordination* (ZSC,

---
*Equal contribution [1]University of Chicago [2]Carnegie Mellon University [3]Common Sense Machines [4]University of Oxford. Correspondence to: Mingwei Ma <mma3@uchicago.edu>.

defined more formally below) in humans predates verbal behavior (Tomasello et al., 2007) and this capability has been hypothesized as a key predecessor to more sophisticated language development and acquisition (Tomasello et al., 2005). Modeling these capacities is key for building machines that can robustly coordinate with other agents and with people (Kleiman-Weiner et al., 2016; Dafoe et al., 2020).

Might this general mechanism emerge through multi-agent reinforcement learning across a range of tasks? As we will show, reinforcement learning agents naively trained with self-play fail to learn to coordinate even in these obvious ways. Instead, they develop arbitrary private languages that are uninterpretable to both the *same* models trained with a different random seed as well as to human partners (Hu et al., 2020). For instance in the examples above, they will be equally likely to wave a red-hat to hint they want strawberries as they would to indicate that they want blueberries.

These problems also emerge at scale in the decentralized partially observable Markov decision process (Dec-POMDP) benchmark Hanabi (Bard et al., 2019). When agents are trained with self-play using standard architectures, they do not develop strategies that take into account the correspondence between the features of the actions (colored and numbered cards) and the observation of the game state (other colored and numbered cards). Unfortunately, developing an inductive bias that might take into account these correspondences is not straightforward because describing the kind of abstract knowledge that these agents lack in closed form is challenging. Rather than attempting to do so, we take a *learning-based* approach. Our aim is to build an agent with the capacity to develop these kinds of abstract correspondences during self-play such that they can robustly succeed during *cross-play*, a process where different models are paired together to play, or during play with humans.

To summarize, our key contributions are:

- We extend the Dec-POMDP formalism to allow actions and observations to be represented using shared features and design a human-interpretable environment for studying coordination with these enrichments.
- We evaluate the role of neural network architectures including feedforward, recurrent, and attention mechanisms on both cross-play generalization and ability to create human-interpretable policies.
- We demonstrate that an attention architecture which takes *both* the action and observations as input allows the agent to exploit the semantic relationships between action and obervation features for coordination, resulting in strong cross-play that outperform baseline ZSC methods.
- We show that the above agents achieve human-level performance when paired with people in a behavioral experiment. The model demonstrates sophisticated human-like coordination patterns that exploit mutual exclusivity and

implicature, two well-known phenomena studied in cognitive science (Markman & Wachtel, 1988; Grice, 1975).

2. Background

Dec-POMDPs. We start with decentralized partially observable Markov decision processes (Dec-POMDPs) to formalize our setting (Nair et al., 2003). In a Dec-POMDP, each player i receives an observation $\Omega^i(s) \in \mathcal{O}^i$ generated by the underlying state s, and takes action $a^i \in \mathcal{A}^i$. Players receive a common reward $R(s, a)$ and the state transitions according to the function $\mathcal{T}(s, a)$. The historical trajectory is $\tau = (s_1, a_1, \ldots, a_{t-1}, s_t)$. Player i's action-observation history (AOH) is denoted as $\tau_t^i = (\Omega^i(s_1), a_1^i, \ldots, a_{t-1}^i, \Omega^i(s_t))$. The policy for player i takes as input an AOH and outputs a distribution over actions, denoted by $\pi^i(a^i \mid \tau_t^i)$. The joint policy is denoted by π.

MARL and Zero-Shot Coordination. The standard paradigm for training multi-agent reinforcement learning (MARL) agents in Dec-POMDPs is self-play (SP). However, the failure of such policies to achieve high reward when evaluated in cross-play (XP) is well-documented. Carroll et al. (2019) used grid-world MDPs to show that both SP and population-based training fail when paired with human collaborators. Bard et al. (2019); Hu et al. (2020) showed that agents perform significantly worse when paired with independently trained agents than they do at training time in Hanabi, even though the agents are trained under identical circumstances. This drop in XP performance directly results in poor human-AI coordination, as shown in (Hu et al., 2020). Lanctot et al. (2017) also find similar qualitative XP results in a partially-cooperative laser tag game.

To address this issue, Hu et al. (2020) introduced the *zero-shot coordination (ZSC) setting, where the goal is to maximize the XP returns of independently trained agents using the same algorithm.*[1] Clearly, good performance in the ZSC setting is a necessary but insufficient condition for successful coordination with humans. If agents trained from independent runs or random seeds using the same algorithm cannot coordinate well with each other, it is unlikely they will be able to coordinate with agents with different model architectures, not to mention humans. Thus formulated, ZSC is an alternative to ad-hoc teamplay, a framework for measuring coordinated team success when faced with players with unknown behavior (Stone et al., 2010; Barrett et al., 2011), which assessed by measuring the average performance of the agent against a distribution of known others.

A few methods have been developed for the ZSC setting.

---

[1]In this work we use the language zero-shot coordination (and the acronym ZSC) technically, as defined above and in previous literature (Hu et al., 2020; 2021), but also colloquially, to mean coordination between agents that did not train together.

other-play (Hu et al., 2020, OP) exploits the symmetries in a given Dec-POMDP to prevent agents from learning permutation equivalent but mutually incompatible policies. Another recent method, off-belief learning (Hu et al., 2021, OBL), regularizes agents' ability to make inferences based on the behavior of others. Compared to prior work on Hanabi in which SP scores were high but XP scores were low, both of OP and OBL improve XP scores and show promising preliminary results in play with humans. However, neither of these algorithms exploit the correspondence between the features of actions and observations as we show in this work.

Dot-Product Attention. As we will see in our experiments, one way to leverage the correspondences between action features and observation features is by using attention mechanisms (Vaswani et al., 2017; Bahdanau et al., 2015; Xu et al., 2016). Given a set of input vectors $(x_1, ..., x_m)$, dot-product attention uses three weight matrices (Q, K, V) to obtain triples (Qx_i, Kx_i, Vx_i) for each $i \in \{1, ..., m\}$, called query vectors, key vectors, and value vectors. We abbreviate these as (q_i, k_i, v_i). Next, for each i, j, dot-product attention computes logits using dot products $q_i \cdot k_j$. These logits are in turn used to compute an output matrix $[\text{softmax}(q_i \cdot k_1 / \sqrt{m}, ..., q_i \cdot k_m / \sqrt{m}) \cdot v_j]_{i,j}$. We denote this output matrix as $\text{Attention}(x_1, ..., x_m)$.

3. Dec-POMDPs with Shared Action and Observation Features

It is common to describe the states and observations in Dec-POMDPs using features, e.g. in card games each card has a rank and a suit. These featurized observations can be exploited by function approximators. In contrast, in typical RL implementations the actions are merely outputs of the neural network and the models do not take advantage of features of the actions. In the standard representation of Dec-POMDPs, actions are defined solely through their effect on the environment through the reward and the state transition functions. In contrast, in real world environments are often grounded and actions can be described with semantic features that refer to the object they act on, e.g. "I pull the *red lever*".

To allow action features to be used by RL agents, we first formalize the concept of observation and action features in Dec-POMDPs. We say a Dec-POMDP has *observation features* if for at least one player i, we can represent the observation $\Omega^i(s)$ as a set of ℓ objects $\Omega^i(s) = \{O_1, ..., O_\ell\}$, where each object $O_j = (f_1, ..., f_{n_j})$ is described by a vector of n_j features. Each of these features f_k exists in a feature space F_k. Similarly, a Dec-POMDP has *action features* if one can factor the representation of the actions into features $a^i = (\hat{f}_1, ..., \hat{f}_m)$, where each action feature $\hat{f}_r \in \hat{F}_r, r = 1, ..., m$, and $\hat{F}_r$ is the action feature space.

In some Dec-POMDPs actions can be described using some

of the *same* features that describe the observations. For example, an agent might observe the "red" light and take the action of pulling the "red" lever where "red" is a shared feature between observations and actions. In such cases there is a *non-empty intersection* between F_k and $\hat{F}_r$ ("shared action-observation features") which may be exploited for coordination. Even in the absence of an exact match, the distance between similar features (e.g., "pink" and "red" and vs. "green" and "red") might also be useful for coordination. We study this possibility in a novel generative environment with action and observation features described next.

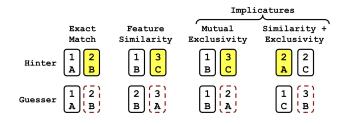## 4. The Hint-Guess Game

Figure 2. Example scenarios in *hint-guess*. Shown above are four hand-crafted scenarios that test distinct dimensions important for ZSC. The highlighted yellow card corresponds to a human-compatible choice. The two right scenarios require agents to reason about implicatures, i.e., the intuitive choice has zero feature overlap with the target card. Model performance in these scenario types is shown in Table 2.

To study Dec-POMDPs with shared action-observation features, we introduce a novel setting that we call *hint-guess*. Hint-guess is a two-player game where players must coordinate to successfully guess a target card. The game consists of a *hinter* and a *guesser*. Both players are given a hand of N cards, $H_1 = \{C_1^1, ...C_N^1\}$ for the *hinter* and $H_2 = \{C_1^2, ...C_N^2\}$ for the *guesser*. Each card has two features (f_1, f_2) where $f_1 \in F_1$ and $f_2 \in F_2$. Cards in each hand are drawn independently and randomly with replacement, with equal probability for any combination of features. Both hands, H_1 and H_2, are public information exposed to both players. Before each game, one of the *guesser's* cards, C_i^2, is randomly chosen to be the target card and its features are revealed to the *hinter*, but not the *guesser*.

In the first round, the *hinter* (who observes H_1, H_2, C_i^2) chooses a card of their own, which we refer to as C_j^1, to show to the *guesser*. In the second round, the *guesser* (who observes H_1, H_2, C_j^1) guesses which of its cards is the target. Both players receive a common reward $r = 1$ if the features of the card played match those of the target, otherwise $r = 0$ for both players.

Fig. 2 shows some simple scenarios that probe key dimensions of coordination with $N = 2$, $F_1 = \{1, 2, 3\}$ and

$F_2 = \{A, B, C\}$. Each of these scenarios has a human-compatible and intuitive solution. The first scenario (exact match) is the most simple—the *hinter* has a copy of the target card (2B) so it can simply hint 2B. The next scenario (feature similarity) requires reasoning about the features under some ambiguity since neither of the cards in the two hands are a direct match. In this case, both cards in the *hinter*'s hand share one feature with the *guesser*. Thus, the human-compatible strategy would be to match the cards that share features to each other. The third and fourth examples (labeled implicatures in Fig. 2) require understanding the action embedded within its context, e.g. what the *hinter* would have done had the goal been different. The third scenario invokes a simple kind of implicature: mutual exclusivity. In this scenario, human-compatible intuitive reasoning follows the logic of: "if the target card *was* 1B, the *hinter* would choose 1B. So that means 1B is taken and 3C should correspond to 2A even though they share no common feature overlap". The final scenario combines feature similarity and mutual exclusivity. These scenarios are particularly interesting as deep learning models often struggle to effectively grapple with mutual exclusivity (Gandhi & Lake, 2020).

5. The Effect of Architecture Choice on Zero-Shot Coordination

We consider the following architectures to investigate the effect of policy parameterization on the agents' ability to exploit shared action and observation features for ZSC. For details about the model architectures, see Appendix A.1.

Feedforward Networks (MLPs). The most basic architecture we test is a standard fully connected feedforward network with ReLU activations. All featurized representation of objects in the observation are concatenated and fed into the network, which outputs the estimated Q-value for each action. There is no explicit representation of action-observation relationships in this model, since observations are inputs and actions are outputs.

Recurrent Networks (LSTMs). We also examine a recurrent model, wherein we feed in objects in the observation (namely, vectors representing cards) sequentially to a long short-term memory (LSTM) network (Hochreiter & Schmidhuber, 1997). To improve trainability we concatenate all hidden states from each step and use them as input to a feedforward neural network, noting that this is unconventional. Like the MLP, the LSTM does not explicitly model the relationship between action and observation features.

Attention (Att). We also investigate three attention-based models as shown in Fig. 3. The first model processes the observations using attention, takes the object-wise mean, and feeds the output into a feedforward network, which
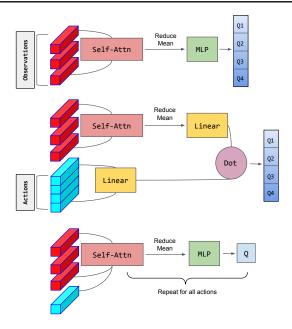

Figure 3. Model architecture for the attention-based models. Top: Attention (Att). Middle: Attention with Linear Constraints (Att + Lin Cons). Bottom: Attention with Action as Input (A2I). The red blocks denote featurized objects in the observation, e.g. cards in the deck. The cyan blocks denote featurized actions, e.g. cards in the hand that can be hinted/guessed. *Self-Attn* and *MLP* denote the attention and fully-connected layers, respectively.

produces a vector with a Q-value for each action

$$Q = \text{MLP}(\text{Mean}(\text{Attention}(O_1, \ldots, O_n)).$$

Attention with Linear Constraints (Att + Lin Cons). The second is setup such that the action-values are constrained to be linear in their features for each decision point. In this model, a linear function of the object-wise mean is multiplied with a linear function of the action feature vectors to produce the values for each action

$$S = \text{Mean}(\text{Attention}(O_1, \ldots, O_n))$$
$$Q = \text{Linear}(S) \cdot \text{Linear}(A).$$

Attention with Action as Input (A2I). Lastly, we look at an attention-based architecture similar to Att, where the featurized action is passed as input to the attention module(s) along with the observations. This outputs a single scalar value at a time, the estimated Q-value for the specific action being fed into the network

$$Q_k = \text{MLP}(\text{Mean}(\text{Attention}(O_1, \ldots, O_n, A_k))).$$

for $k = 1, \ldots, m$. To be clear, this architecture requires a forward pass for each action to calculate the Q-value vector.

6. Experiment Setup

We experimentally evaluate the architectures in the hint-guess game introduced in Section 4. In Sections 7.1-7.3, we fix the hand size to be $N = 5$ and the features to be $F_1 = \{1, 2, 3\}$ and $F_2 = \{A, B, C\}$. [2] We use a one-hot encoding for features; more specifically, we use a two-hot vector to represent the two features of each card. In Sec. 7.4-7.5, we examine a qualitatively different version of the game where $N = 3$ and there is only one feature, $F_1 = \{0, 1, ..., 19\}$. In this version, we investigate whether it is possible to capture ordinal relationships between actions using sinusoidal positional encodings. For these experiments, we encode each number as a 200-dimensional vector consisting of sine and cosine functions of different frequencies, following the procedure of Vaswani et al. (2017).

For both variants of the game, the observation input is a sequence of card representations for both hands H_1 and H_2, as well as the representation of the target card, C_i^2 (for the *hinter*) or the hinted card C_j^1 (for the *guesser*), and we train agents in the standard self-play setting using independent Q-learning (Tan, 1993, IQL), where the *hinter* and *guesser* are jointly trained to maximize their score in randomly initialized games. To avoid giving the set-based attention architectures an unfair advantage, we also permute the cards in the hands observed by all agents so that agents are not able to coordinate using the position of the cards. To evaluate success, we consider the agents' performance and behavior in both SP and the ZSC setting. We also provide fine-grained examination of their policies and investigate their ability to match the human-compatible response in different scenarios. See Appendix A.1 for training details.

7. Result Analysis

7.1. Cross-play Performance.

First, we evaluate model cross-play (XP) performance for each architecture in the ZSC setting. In this setting, agents from independent training runs with different random seeds are paired together. Fig. 4 records the scores obtained by each pair of agents, where the diagonal entries are the within-pair SP scores and the off-diagonal entries are XP scores. Table 1 summarizes average SP and XP scores across agents.

Comparison Across Architectures. Fig. 4 shows that the XP matrix of all architectures except A2I (Attention with Action as Input) lack an interpretable pattern. The XP score is near chance for these architectures as shown in Table 1. In contrast, the XP matrix for the A2I model shows two clear clusters. Within the clusters, agents show XP perfor-

---

[2]There is nothing particular about the hand size, and as shown in Appendix A.5, similar results can be obtained with either a larger or smaller hand size.

mance nearly identical to that of their SP, implying that they coordinate nearly perfectly with other agents trained with a different seed, whereas outside the clusters they achieve a return close to zero.

As we will show in the next section, the upper cluster, which has a higher average XP score, corresponds to a highly interpretable and human-like strategy where agents *maximize* the "similarity" between the target and the hint card (as well as between the hint card and the guess card). In the lower, second cluster, agents do the opposite. They try to hint/guess cards that share no common feature with the target/hint cards. In the rest of the paper, we will refer to the cluster where agents maximize the similarity between cards as **A2I Sim**, and the cluster where agents maximize the dissimilarity as **A2I Dissim**. However, as we will see in section 7.2, the A2I agents do not just maximize/minimize feature similarity; they also demonstrate more sophisticated coordination patterns that exploit implicature.

Model Architectures		
Model	Cross-Play	Self-Play
MLP	0.27 ± 0.04	0.85 ± 0.02
LSTM	0.30 ± 0.05	0.86 ± 0.01
Att	0.27 ± 0.04	0.87 ± 0.01
Att + Lin Cons	0.26 ± 0.03	0.76 ± 0.02
A2I	0.37 ± 0.12	0.76 ± 0.02
A2I Sim	0.77 ± 0.01	0.82 ± 0.01
A2I Dissim	0.71 ± 0.01	0.72 ± 0.01

Baseline Training Algorithms		
Algothrim	Cross-Play	Self-Play
OP	0.35 ± 0.02	0.35 ± 0.02
OBL (level 1)	0.27 ± 0.05	0.29 ± 0.06
OBL (level 2)	0.28 ± 0.04	0.28 ± 0.05

Table 1. Cross-play performance. Each entry is the average performance of 20 pairs of agents that are trained with different random seeds. The XP score is the off-diagonal mean of each grid. The SP score is the diagonal mean, i.e. the score attained when agents play with the peer they are trained with. A "chance agent" that acts randomly is expected to obtain a score of 0.28. All models in the "Model Architecture" part are trained with IQL (Tan, 1993), and all training algorithms in the "Baseline Training Algorithm" section use an MLP architecture.

Comparison with ZSC Baselines. The bottom part of Table 1 contains the SP and XP results for two recent ZSC algorithms, other-play (Hu et al., 2020, OP) and off-belief learning (Hu et al., 2021, OBL). For details and implementation of the baseline algorthims, see Appendix A.3.

As shown, the XP scores for OP agents only show marginal improvement over MLP agents. By preventing arbitrary symmetry breaking, OP improves XP performance, but only to a limited extent. In contrast, the OBL agents fail to

obtain scores beyond chance both in XP and SP. This is expected as OBL is designed to explicitly prevent *cheap talk*, i.e., sending costless messages between players, which is exactly the key for coordination in hint-guess.

7.2. Policy Examination

Conditional Probability Analysis. In Fig. 5, we provide the conditional probability for the *guesser* to guess a card given the hinted card (bottom row). [3] One crucial thing to analyze is whether agents assign different probabilities to actions based on the features they share with the observation. One can see that for MLP, LSTM and Att, the probability matrices for both target-hint and hint-guess are nearly uniform. This implies that the SP policies across seeds each form their own private language for arbitrary and undecipherable coordination. While Att + Lin Cons shows some preference for actions that share one or two features with the observations, the probability matrix remains noisy.

In contrast, for the two clusters of A2I agents the correlation (or anti-correlation) between the action features and target/hint card features is much stronger. For A2I Sim, both the *hinter* and the *guesser* prioritize exact matches when they are present. If the exact match is not present, they turn to cards that share one feature in common. The A2I Dissim agents do the exact opposite—matching cards together that share as few features as possible.

Human Compatibility Analysis. However, we find that the nuance with which these clusters play goes beyond simply maximizing or minimizing feature similarity. To demonstrate this, we run simulations on the four scenarios (exact match, feature similarity, mutual exclusivity, exclusivity+similarity) shown in Fig. 2 and described in Section 4. In Table 2, we record the percentage of times where A2I agents in each cluster chose the human-compatible actions in Fig. 2. We find that A2I Sim agents demonstrate coordination patterns that are nearly identical to a human-compatible policy. These results are surprising given that our models have never been trained with any human data. Furthermore, mutual exclusivity was thought to be hard for deep learning models to learn (Gandhi & Lake, 2020). In contrast, A2I Dissim agents always perform actions that are the *opposite* to the human-compatible policy, but this policy *per se* is still interpretable and non-arbitrary.

7.3. Human-AI Experiments

We recruited 10 university students to play hint-guess. Each subject played as *hinter* for 15 randomly generated games, totaling 150 different games. These subjects are then cross-matched to play as *guessers* with the hints their peers generated. The human hints are also fed into randomly sampled MLP and A2I Sim *guesser*-agents to test AI performance against human partners. The experiment was carefully designed so that the hinter is never informed of the guesser's guess and the guesser is never informed of the true target card. This experimental design ensures that the human participants generate zero-shot data, and do not optimize their play using previous experience. Further details of the experiment are in Appendix A.2.

ZSC Performance. In the right table of Fig. 6 we report average zero-shot coordination (ZSC) scores obtained by *hinter-guesser* pairs for human-human, human-MLP, and human-A2I Sim. Humans obtained an average ZSC score of 0.75 with their peers. As a baseline, the MLP *guessers* show poor performance in understanding human-generated hints, barely outperforming random guessing. In contrast, the A2I Sim *guessers* achieve human-level performance with an average ZSC score of 0.77 with humans. Note that this score is very close to the average ZSC score in Table 1, where A2I Sim agents cross-played among themselves.

Human-AI Behavior Correlation. We also investigate two kinds of correlations between human play and AI play. The right table of Fig. 6 shows the percentage of games where model *guessers* chose the same action as the human *guessers*. In 80.7% of the games, the A2I Sim agents and human *guessers* agree on the same action across many different scenarios. In contrast, the MLP *guessers* deviate from human *guessers*, with only 40.7% agreement.

Human-AI Performance Correlation. The left plot of Fig. 6, shows the correlations between human-human play and human-AI play. As expected, across humans we observed a range of skill levels at the game, with some hinters not even achieving 50% guess accuracy when paired with other humans, while others exceeded 90% (as measured along the x-axis). We observe the performance of human-A2I Sim pairs increased substantially with the skill level of the human, whereas the performance of human-MLP pairs was less sensitive along this axis. Taken together, these results suggest that the A2I Sim agent is both better at coordinating with people than a baseline model and is also better at coordinating with the people who are better at coordinating with people.

7.4. Sinusoidal Encoding

The previous subsections investigated a variant of hint-guess in which the most important mode of comparison between features was whether they were equal or non-equal. In these settings the A2I models were able to learn sophisticated cognitive patterns like mutual exclusivity from one-hot encoding of inputs. However, one-hot encoding does not capture richer semantic relationships between features. For instance, in hint-guess, if cards are encoded one-hot, the agent can

---

[3]The conditional probability matrices for the *hinter* to hint a card for given target card look exactly identical so we omit them.
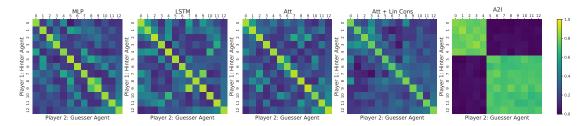
Figure 4. Cross-play matrices. Visualization of paired evaluation of different agents trained under the same method. The y-axis represents the agent index of the *hinter* and the x-axis represents the agent index of the *guesser*. Each block in the grid is obtained by evaluating the pair of agents on 10K games with different random seeds. Numerical performance is shown in Table 1.
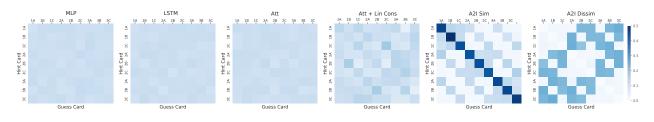

Figure 5. Conditional probability matrices. We show $\Pr(\text{Guess}|\text{Hint})$, for the *guesser* to guess a particular card (x-axis) when the hinted card is the card on the y-axis. Each subplot is the sample average of 20 agent-pairs with different seeds for 1K games within pair.
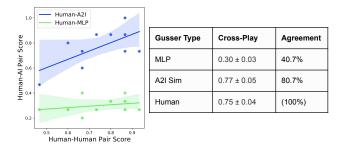

Figure 6. Human-AI ZSC results comparing human-human pairs, human-A2I Sim pairs and human-MLP pairs. In the left plot, each point corresponds to a particular human hinter. In the table, "agree" measures the percentage of games in which the guesser selected the same card as the human guesser.

Gusser Type	Cross-Play	Agreement
MLP	0.30 ± 0.03	40.7%
A2I Sim	0.77 ± 0.05	80.7%
Human	0.75 ± 0.04	(100%)

only "know" that the card 1A has the same first label as the card 1B, but it cannot "know" whether the number 1 is closer to 2 than to 5. Thus, in this section, we investigate whether a more expressive encoding enables the A2I model to learn to leverage the ordinal relationship between features. Specifically, we examine the performance of sinusoidal positional encodings in a variant of hint-guess in which the only card feature is a number between 0 and 19, as described in the experiment setup.

We show the results of this experiment in Table 3, which shows SP and XP performance of A2I agents with one-hot encoding and sinusoidal encoding in this single-feature setting. Agents with one-hot encoding are near chance in XP. They do not form clusters as observed before. We hypothe-

size that the failure of one-hot agents is because of the large feature space (20 numbers) relative to the small number of features (1). Because the feature space is large and the agents are only sensitive to exact overlap, the performance gain in SP is marginal. Thus, one-hot agents degenerate into using arbitrary conventions, resulting in a large performance gap between SP and XP.

Agents with sinusoidal encodings, in contrast, split into two clusters (named A2I Sim and A2I Dissim as before), wherein each cluster has near-perfect SP and XP scores with no significant performance gap. We find that these agents learn to exploit the ordering and distance information between the numbers for coordination. A2I Sim agents rank the *hinter*'s and *guesser*'s hands in the same order and match the corresponding numbers as hint-guess pairs. A2I Dissim agents, on the other hand, rank one hand in ascending order and the other hand in descending order for matching. See Fig. 7 for a concrete example. For both strategies, if the hinter does not have duplicate numbers in its hand, agents obtain a near-perfect play score.

Indeed, in a XP simulation across 15 agent-pairs with 1K games per pair, where each agent's hand is drawn *without replacement* (so no duplicates), in 99.9% of the time, the A2I Sim agents hint/guess exactly according to the same order matching scheme. Also in 99.9% of the time, the A2I Dissim agents hint/guess according to the reversed order matching scheme.

Scenario	Self-Play (A2I Sim)		Cross-Play (A2I Sim)		Self-Play (A2I Dissim)		Cross-Play (A2I Dissim)	
	Human (%)	Win (%)	Human (%)	Win (%)	Human (%)	Win (%)	Human (%)	Win (%)
Exact match	100.0	100.0	100.0	100.0	0.0	100.0	0.0	100.0
Feature similarity	100.0	100.0	100.0	100.0	0.0	100.0	0.0	100.0
Mutual exclusivity	100.0	100.0	100.0	100.0	9.3	91.2	9.3	92.2
Similarity + Exclusivity	92.0	91.7	97.9	99.5	3.2	98.4	0.0	99.9

Table 2. Behavioral analysis for the A2I model in the Fig. 2 scenarios. We randomly chose 20 agent-pairs from each cluster and simulated the same scenario 1K times. Human (%) denotes the fraction of games where the *hinter* hints the card that corresponds to human-compatible choice (highlighted in yellow in Fig. 2), and Win (%) denotes the fraction where the *guesser* correctly guesses.

Encoding	SP	XP	XP (A2I Sim)	XP (A2I Dissim)
One-hot	0.81 ± 0.02	0.36 ± 0.10	-	-
Sinusoidal	0.92 ± 0.01	0.52 ± 0.16	0.92 ± 0.01	0.93 ± 0.01

Table 3. SP and XP scores for A2I agents with one-hot and sinusoidal encodings. Agents with sinusoidal encoding form two clusters so we also show the within-cluster results.
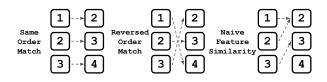

Figure 7. A scenario illustrating the behavior of A2I agents. In this scenario, the *hinter*'s hand is $(1, 2, 3)$ and the *guesser*'s hand is $(2, 3, 4)$ (the actual hands seen by agents will be permuted). We find that with probability close to 1, A2I Sim agents use a strategy that exploits *same order matching* (left). They sort both hands in the same order and match 1-2, 2-3, 3-4, etc. Also with probability close to 1, A2I Dissim agents use *reversed order matching* (middle). They sort one hand in ascending order and the other in descending order and match. To compare we also show *naive feature similarity* (right) that solely maximizes feature similarity; this strategy will match 1-2, 2-2, 3-3 and leave out 4.

7.5. Multi-head and Multi-layer Attention

We also find that the results for A2I architectures are qualitatively similar when using multi-head or multi-layer attention or both in Appendix A.4. This suggests that A2I may also be able to produce human-compatible policies in settings where larger architectures are required for effective learning.

8. Related Work

Attention for Input-Output Relationships. Exploiting semantic relationships between inputs and outputs via an attention-based model has been studied in the deep learning literature. In natural language processing, such an idea is commonly used in question answering models (dos Santos et al., 2016; Tan et al., 2016; Yang et al., 2016). For instance, Yang et al. (2016) form a matrix that represents the semantic matching information of term pairs from a question and answer pair, and then use dot-product attention to model

question term importance. For regression tasks, Kim et al. (2019) proposed attentive neural processes (ANP) that use dot-product attention to allow each input location to attend to the relevant context points for the prediction, and applied ANP to vision problems.

Human Coordination. Our work is also inspired by how humans coordinate in cooperative settings. Theory-of-mind, the mechanism people use to infer intentions from the actions of others, plays a key role in structuring coordination (Wu et al., 2021; Shum et al., 2019). In particular, rational speech acts (RSA) is a influential model of pragmatic implicature (Frank & Goodman, 2012; Goodman & Stuhlmüller, 2013). At the heart of these approaches are probabilistic representations of beliefs that allow for modeling uncertainty and recursive reasoning about the beliefs of others, enabling higher-order mental state inferences. This recursive reasoning step also underlies the cognitive hierarchy and level-K reasoning models, and is useful for explaining certain focal points (Camerer, 2011; Stahl & Wilson, 1995; Camerer et al., 2004). However, constructing recursive models of players beliefs and behavior is computationally expensive as each agent must construct an exponentially growing number of models of each agent modeling each other agent. As a result, recursive models are often limited to one or two levels of recursion. Furthermore, none of these approaches can by itself take advantage of the shared features across actions and observations.

9. Conclusion

We investigated the effect of network architecture on the ability of learning algorithms to exploit the semantic relationship between shared features across actions and observations for coordination, comparing the behavior of agents with feedforward, recurrent, and attention-based architectures. We found that that attention-based architectures that jointly process a featurized representation of observations and actions have a better inductive bias for exploiting this relationship. Our results suggest that this is a promising architecture to investigate for more complex games in the zero-shot coordination setting, like Hanabi or Overcooked (Wu et al., 2021; Carroll et al., 2019).

References

Bahdanau, D., Cho, K., and Bengio, Y. Neural machine translation by jointly learning to align and translate. *International Conference on Learning Representations*, 2015.

Bard, N., Foerster, J. N., Chandar, S., Burch, N., Lanctot, M., Song, H. F., Parisotto, E., Dumoulin, V., Moitra, S., Hughes, E., Dunning, I., Mourad, S., Larochelle, H., Bellemare, M. G., and Bowling, M. The hanabi challenge: A new frontier for ai research. *Artificial Intelligence*, 2019. doi: 10.1016/j.artint.2019.103216.

Barrett, S., Stone, P., and Kraus, S. Empirical evaluation of ad hoc teamwork in the pursuit domain. In *AAMAS*, pp. 567–574, 2011.

Camerer, C. F. *Behavioral game theory: Experiments in strategic interaction*. Princeton university press, 2011.

Camerer, C. F., Ho, T.-H., and Chong, J.-K. A cognitive hierarchy model of games. *The Quarterly Journal of Economics*, 119(3):861–898, 2004.

Carroll, M., Shah, R., Ho, M. K., Griffiths, T., Seshia, S., Abbeel, P., and Dragan, A. On the utility of learning about humans for human-ai coordination. *Advances in Neural Information Processing Systems*, 32:5174–5185, 2019.

Dafoe, A., Hughes, E., Bachrach, Y., Collins, T., McKee, K. R., Leibo, J. Z., Larson, K., and Graepel, T. Open problems in cooperative ai. *arXiv preprint arXiv:2012.08630*, 2020.

dos Santos, C. N., Tan, M., Xiang, B., and Zhou, B. Attentive pooling networks. *CoRR*, abs/1602.03609, 2016. URL http://arxiv.org/abs/1602.03609.

Frank, M. C. and Goodman, N. D. Predicting pragmatic reasoning in language games. *Science*, 336(6084):998–998, 2012.

Gandhi, K. and Lake, B. M. Mutual exclusivity as a challenge for deep neural networks. *Advances in Neural Information Processing Systems*, 33, 2020.

Goodman, N. D. and Stuhlmüller, A. Knowledge and implicature: Modeling language understanding as social cognition. *Topics in cognitive science*, 5(1):173–184, 2013.

Grice, H. P. Logic and conversation. In *Speech acts*, pp. 41–58. Brill, 1975.

Hochreiter, S. and Schmidhuber, J. Long short-term memory. *Neural Comput.*, 9(8):1735–1780, November 1997. ISSN 0899-7667. doi: 10.1162/neco.1997.9.8.1735. URL https://doi.org/10.1162/neco.1997.9.8.1735.

Hu, H., Lerer, A., Peysakhovich, A., and Foerster, J. "Other-Play" for Zero-Shot Coordination. *International Conference on Machine Learning*, 2020.

Hu, H., Lerer, A., Cui, B., Pineda, L., Wu, D., Brown, N., and Foerster, J. Off-belief learning. *International Conference on Machine Learning*, 2021.

Kim, H., Mnih, A., Schwarz, J., Garnelo, M., Eslami, A., Rosenbaum, D., Vinyals, O., and Teh, Y. W. Attentive neural processes. *International Conference on Learning Representations*, 2019.

Kleiman-Weiner, M., Ho, M. K., Austerweil, J. L., Littman, M. L., and Tenenbaum, J. B. Coordinate to cooperate or compete: abstract goals and joint intentions in social interaction. In *CogSci*, 2016.

Köhler, W. *Gestalt psychology*. Liveright, 1929.

Lanctot, M., Zambaldi, V. F., Gruslys, A., Lazaridou, A., Tuyls, K., Pérolat, J., Silver, D., and Graepel, T. A unified game-theoretic approach to multiagent reinforcement learning. In *NIPS*, 2017.

Lerer, A. and Peysakhovich, A. Learning social conventions in markov games. *arXiv preprint arXiv:1806.10071*, 2018.

Lewis, D. K. *Convention: A Philosophical Study*. Blackwell, 1969.

Markman, E. M. and Wachtel, G. F. Children's use of mutual exclusivity to constrain the meanings of words. *Cognitive Psychology*, pp. 121–157, 1988.

Maurer, D., Pathman, T., and Mondloch, C. J. The shape of boubas: Sound–shape correspondences in toddlers and adults. *Developmental science*, 9(3):316–322, 2006.

Misyak, J. B., Melkonyan, T., Zeitoun, H., and Chater, N. Unwritten rules: virtual bargaining underpins social interaction, culture, and society. *Trends in cognitive sciences*, 18(10):512–519, 2014.

Nair, R., Tambe, M., Yokoo, M., Pynadath, D., and Marsella, S. Taming decentralized pomdps: Towards efficient policy computation for multiagent settings. *International Joint Conferences on Artificial Intelligence*, pp. 705–711, 2003.

Pal, A., Philion, J., Liao, Y.-H., and Fidler, S. Emergent road rules in multi-agent driving environments. In *International Conference on Learning Representations*, 2020.

Shum, M., Kleiman-Weiner, M., Littman, M. L., and Tenenbaum, J. B. Theory of minds: Understanding behavior in groups through inverse planning. In *Proceedings of the AAAI conference on artificial intelligence*, volume 33, pp. 6163–6170, 2019.

Stahl, D. O. and Wilson, P. W. On playerśmodels of other players: Theory and experimental evidence. *Games and Economic Behavior*, 10(1):218–254, 1995.

Stone, P., Kaminka, G. A., Kraus, S., and Rosenschein, J. S. Ad hoc autonomous agent teams: Collaboration without pre-coordination. In *Twenty-Fourth AAAI Conference on Artificial Intelligence*, 2010.

Tan, M. Multi-agent reinforcement learning: Independent vs. cooperative agents. *Proceedings of the tenth international conference on machine learning*, pp. 330–337, 1993.

Tan, M., Dos Santos, C., Xiang, B., and Zhou, B. Improved representation learning for question answer matching. *Annual Meeting of the Association for Computational Linguistics (ACL)*, pp. 464–473, 01 2016. doi: 10.18653/v1/P16-1044.

Tomasello, M., Carpenter, M., Call, J., Behne, T., and Moll, H. Understanding and sharing intentions: The origins of cultural cognition. *Behavioral and brain sciences*, 28(5): 675–691, 2005.

Tomasello, M., Carpenter, M., and Liszkowski, U. A new look at infant pointing. *Child development*, 78(3):705–722, 2007.

Vaswani, A., Shazeer, N., Parmar, N., Uszkoreit, J., Jones, L., Gomez, A. N., Kaiser, L., and Polosukhin, I. Attention Is All You Need. *Advances in Neural Information Processing Systems*, 2017.

Wu, S. A., Wang, R. E., Evans, J. A., Tenenbaum, J. B., Parkes, D. C., and Kleiman-Weiner, M. Too many cooks: Bayesian inference for coordinating multi-agent collaboration. *Topics in Cognitive Science*, 13(2):414–432, 2021.

Xu, K., Ba, J., Kiros, R., Cho, K., Courville, A., Salakhutdinov, R., Zemel, R., and Bengio, Y. Show, attend and tell: Neural image caption generation with visual attention. *International Conference on Machine Learning*, 2016.

Yang, L., Ai, Q., Guo, J., and Croft, W. B. anmm: Ranking short answer texts with attention-based neural matching model. *Proceedings of the 25th ACM International on Conference on Information and Knowledge Management*, 2016.

Young, H. P. The evolution of conventions. *Econometrica: Journal of the Econometric Society*, pp. 57–84, 1993.

A. Appendix

A.1. Training and Model Architecture Details

Training Setup. By default we use standard experience-replay with a replay memory of size 300K. For optimization, we use the mean squared error loss, stochastic gradient descent with learning rate set to 10^{-4} and minibatches of size 500 each. We train the agents using 4M episodes. To allow more data to be collected between training steps, we update the network only after we receive 500 new observations rather than after every observation. We use the standard exponential decay scheme with exploration rate $\epsilon = \epsilon_m + (\epsilon_0 - \epsilon_m) \exp(-n/K)$, where n is the number of episodes, $\epsilon_m = 0.01$, $\epsilon_0 = 0.95$, and $K = 50,000$. All experiments were run on two computing nodes with 256GB of memory and a 28-Core Intel 2.4GHz CPU. A single training run takes roughly 8 hours for the A2I model and 2 hours for all other models. All *hinters* and *guessers* have the same model structure.
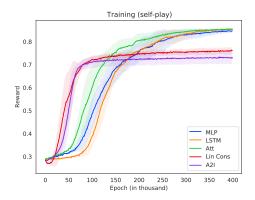

Figure 8. Training performance of different architectures for hint-guess. The x-axis is the number of episodes and y-axis is the mean training reward. Solid line is the mean, shading is the standard error of the mean (s.e.m) across 20 different seeds.

The model architecture details are as follows:

Feedforward Networks (MLP). The MLP agent is a feedforward ReLU neural network with 3 hidden layers (width 128).

Recurrent Networks (LSTM). The LSTM agent has an LSTM layer with 128 LSTM units followed by two fully-connected layers with 128 ReLU units. The input of the LSTM agent is the same as that of the MLP agent but vectors representing the cards are fed in sequentially to the LSTM before we concatenate all hidden states from each step and use that as input to a feedforward neural network.

Attention Models. All three attention-based models share the same single-head attention layer with size determined by the shapes of the input and output. By default we do not add position encoding. In Att and A2I, we add a feedforward ReLU MLP with 3 hidden layers (width 128 each) after the attention layer. In $\text{Att} + \text{Lin Cons}$, we add fully-connected layers with conformable dimensions but do not add extra ReLU activation.

A.2. Design of Human-AI Experiments

In this section we provide details of the design of human-based experiments.

We recruited 10 individuals who are undergraduate and master students at a university. The instructions they received include: (i) rules of hint-guess; (ii) that they need to assume they are playing against a *guesser* who is an ordinary human (they are not told that they would play against AI bots); (iii) that the position of the cards are permuted so they cannot provide/interpret hints based on card position, and (iv) if two cards have the same features they are effectively the same.

After they showed understanding of the instructions, the subjects were asked to act as *hinters*. Each subject was provided with 15 randomly generated games with $F_1 = \{1, 2, 3\}$, $F_2 = \{A, B, C\}$ and $N = 5$. They were presented with both hands and the target card and were asked to write down their hints. A sample question they received was:

```
            Playable card is:  2B
   Your (hinter) hand is:  1C, 1B, 3B, 2C, 1A
       Guesser hand is:  1B, 2C, 2B, 2C, 2B
Please choose a hint card from YOUR OWN hand!
```

After the subjects provided hints, they were given no feedback to ensure that they could not learn about the agent they are playing with; this would ensure that their actions are zero-shot.

Then we used the hints provided by the subjects to obtain human-human (*hinter-guesser*) and human-AI scores. To obtain human/human scores, we randomly mix-matched the subjects so that each subject would now act as the *guesser* for 15 games generated by another human subject. This time, they were provided with both hands and the human hint, and were ask to choose one card to play. Same as before, they did not receive any feedback about their guesses to ensure zero-shot.

To obtain human-A2I Sim and human- MLP scores, we reproduced the 150 games and fed human hints to randomly sampled A2I Sim-MLP *guesser* agents.

A.3. Details of ZSC Baselines

In this section we provide implementation details of other-play (Hu et al., 2020) and off-belief learning (Hu et al., 2021), two recent zero-shot coordination (ZSC) methods that we use as baselines.

Other-play (OP). The goal of OP is to find a strategy that is robust to partners breaking symmetries in different ways. To achieve this, it uses reinforcement learning to maximize returns when each agent is matched with agents playing the same policy, but under a random relabeling of states and actions under known symmetries of the Dec-POMDP (Hu et al., 2020). To apply OP, we change the objective function of the hinter from the standard self-play (SP) learning rule objective

$$\pi^* = \arg\max_\pi J\left(\pi^1, \pi^2\right) \tag{1}$$

To the OP objective

$$\pi^* = \arg\max_\pi \mathbb{E}_{\phi \sim \Phi} J\left(\pi^1, \phi\left(\pi^2\right)\right) \tag{2}$$

where the expectation is taken with respect to a uniform distribution on Φ, where Φ describes the symmetries in the underlying Dec-POMDP (in the hint-and-play games, the symmetries are the two features).

As OP only changes the objective function, it can be applied on top of any SP algorithm. We choose to apply OP on top of the MLP architecture, using the same training method as detailed in Appendix. A.1, and change the objective to the OP objective. In implementation, this means that the guesser will receive a feature-permuted version of the game, i.e. feature 1 and feature 2 (the letters and the numbers) of the hands and the hint that the guesser receives will be a permuted version of what the hinter originally receives.

Off-belief learning (OBL). OBL (Hu et al., 2021) regularizes agents' ability to make inferences based on the behavior of others by forcing the agents to optimize their policy π_1 assuming past actions were taken by a given fixed policy π_0, while in the same time assuming that future actions will be taken by π_1. In practice, OBL can be iterated in a hierarchical order, where the optimal policy from the lower level becomes the input to the next higher level.

We apply OBL on MLP agents and keep the training setup the same as in Appendix A.1. At the lowest level (level 1), OBL agents assume π_0 is the policies where actions are chosen uniformly at random. And OBL level 2 assumes the policy from OBL level 1 is the new π_0, and so forth.

A.4. Multi-head and Multi-layer Attention

We show the XP results when using the A2I architecture with different number of attention heads or attention layers. We also show the same results for using either one-hot or sinusoidal encoding. To enable using sinusoidal encoding, we fix the hand size $N = 3$ and only use one feature, $F_1 = \{0, 1, ..., 19\}$, which is equivalent to fixing $F_2 = \{A\}$.

For these experiments we use standard experience-replay with a replay memory of size 1K. For optimization, we use the mean squared error loss, stochastic gradient descent with learning rate set to 10^{-4} and minibatches of size 200 each. We train the agents using 5M episodes. To allow more data to be collected between training steps, we update the network only after we receive 50 new observations rather than after every observation. We use the standard exponential decay scheme with exploration rate $\epsilon = \epsilon_m + (\epsilon_0 - \epsilon_m) \exp(-n/K)$, where n is the number of episodes, $\epsilon_m = 0.05$, $\epsilon_0 = 0.95$, and $K = 15,000$. All experiments were run on two computing nodes with 256GB of memory and a 28-Core Intel 2.4GHz CPU. A single training run takes roughly 6 hours for 1-layer attention and 18 hours for 3-layer attention. All *hinters* and *guessers* have the same model structure.

Encoding	Layers	Heads	SP	XP	XP (Clus. 1)	XP (Clus. 2)
One-hot	1	1	0.81 ± 0.02	0.36 ± 0.10	-	-
One-hot	1	4	0.90 ± 0.02	0.36 ± 0.10	-	-
One-hot	3	1	0.40 ± 0.04	0.38 ± 0.14	-	-
One-hot	3	4	0.89 ± 0.05	0.36 ± 0.11	-	-
Sinusoidal	1	1	0.92 ± 0.01	0.52 ± 0.16	0.92 ± 0.01	0.93 ± 0.01
Sinusoidal	1	4	0.92 ± 0.01	0.67 ± 0.13	0.92 ± 0.01	0.93 ± 0.01
Sinusoidal	3	1	0.94 ± 0.01	0.56 ± 0.16	0.95 ± 0.01	0.91 ± 0.01
Sinusoidal	3	4	0.96 ± 0.01	0.76 ± 0.09	0.95 ± 0.01	0.95 ± 0.01

Table 4. Robustness results for using multi-head and multi-layer attention. We show SP and XP scores for A2I agents with different number of attention modules (layers), attention heads, and different encoding of features. Each entry is the average performance is of 20 pairs of agents that are trained with different random seeds. Agents with sinusoidal encoding forms two clusters so we also show the within-cluster results.

A.5. Effect of Hand Size on Performance

In this section we analyze the effect of hand size on agents' self-play and cross-play performance. We fix the features to be $F_1 = \{1, 2, 3\}$ and $F_2 = \{A, B, C\}$ and run experiments with hand size $N = \{3, 7\}$, as opposed to $N = 5$ in the main text. As shown in the following Table 5, SP and XP results largely confirm our findings for $N = 5$. We also show the same results for a simplified version of the game, where both *hinter* and *guesser* have the same hand. In the simplified game, an optimal and intuitive strategy exists, which is to always hint the target card and then guess the card that is hinted. The training setup and model details are exactly the same as in A.1.

Method	Full Game ($N = 3$)		Same Hand Condition	
	Cross-Play	Self-Play	Cross-Play	Self-Play
MLP	0.47 ± 0.06	0.92 ± 0.01	0.87 ± 0.04	0.98 ± 0.02
LSTM	0.47 ± 0.07	0.92 ± 0.01	0.70 ± 0.04	0.99 ± 0.01
Att	0.47 ± 0.06	0.92 ± 0.01	0.47 ± 0.05	0.95 ± 0.01
Att + Lin Cons	0.38 ± 0.05	0.81 ± 0.01	0.46 ± 0.06	0.88 ± 0.04
A2I	0.43 ± 0.12	0.80 ± 0.01	0.45 ± 0.18	0.95 ± 0.02
A2I Sim	0.81 ± 0.01	0.81 ± 0.01	1.00 ± 0.00	1.00 ± 0.00
A2I Dissim	0.80 ± 0.01	0.80 ± 0.01	0.89 ± 0.02	0.90 ± 0.01
OP	0.55 ± 0.03	0.54 ± 0.04	0.90 ± 0.01	0.98 ± 0.01
OBL (level 1)	0.47 ± 0.07	0.44 ± 0.06	0.47 ± 0.03	0.48 ± 0.03
OBL (level 2)	0.47 ± 0.04	0.46 ± 0.06	0.47 ± 0.05	0.47 ± 0.05

Method	Full Game ($N = 7$)		Same Hand Condition	
	Cross-Play	Self-Play	Cross-Play	Self-Play
MLP	0.22 ± 0.08	0.72 ± 0.03	0.77 ± 0.10	0.96 ± 0.08
LSTM	0.25 ± 0.09	0.76 ± 0.01	0.62 ± 0.14	0.95 ± 0.05
Att	0.24 ± 0.09	0.77 ± 0.03	0.24 ± 0.08	0.93 ± 0.01
Att + Lin Cons	0.22 ± 0.11	0.77 ± 0.02	0.22 ± 0.13	0.80 ± 0.09
A2I	0.37 ± 0.33	0.70 ± 0.06	0.40 ± 0.38	0.89 ± 0.11
A2I Sim	0.78 ± 0.01	0.78 ± 0.03	1.00 ± 0.00	1.00 ± 0.00
A2I Dissim	0.67 ± 0.02	0.67 ± 0.02	0.67 ± 0.03	0.67 ± 0.02
OP	0.32 ± 0.02	0.31 ± 0.02	0.79 ± 0.02	0.95 ± 0.02
OBL (level 1)	0.21 ± 0.04	0.22 ± 0.03	0.22 ± 0.03	0.22 ± 0.04
OBL (level 2)	0.24 ± 0.03	0.22 ± 0.03	0.22 ± 0.03	0.25 ± 0.02

Table 5. Cross-play performance for card number $N = 3$ and $N = 7$. We show results for both the full hint-guess game and the simplified version where both agents have the same hand. Each entry is the average performance is of 20 pairs of agents that are trained with different random seeds. Cross-Play score is the nondiagonal mean of each grid. Self-Play score is the diagonal mean, i.e. the score attained when agents play with the peer they are trained with.